Published in final edited form as:
Biol Blood Marrow Transplant. 2014 October ; 20(10): 1592–1598. doi:10.1016/j.bbmt.2014.06.014.

Parametric Response Mapping as an Indicator of Bronchiolitis Obliterans Syndrome following Hematopoietic Stem Cell Transplantation

Craig J. Galbán, PhD[1], **Jennifer L. Boes, PhD**[1], **Maria Bule**[1], **Carrie L Kitko, MD**[2,3], **Daniel R Couriel, MD**[2,4], **Timothy D. Johnson, PhD**[5], **Vihba Lama, MD**[4], **Eef D. Telenga, MD**[7], **Maarten van den Berge, MD**[7], **Alnawaz Rehemtulla, MD**[6], **Ella A. Kazerooni, MD**[1], **Michael J. Ponkowski**[2], **Brian D. Ross, PhD**[1], and **Gregory A. Yanik, MD**[2,3,4]

[1]Department of Radiology, University of Michigan, Ann Arbor, Michigan 48109, USA [2]Department of Blood and Marrow Transplant Program, University of Michigan, Ann Arbor, Michigan 48109, USA [3]Department of Pediatrics and Communicable Diseases, University of Michigan, Ann Arbor, Michigan 48109, USA [4]Department of Internal Medicine, University of Michigan, Ann Arbor, Michigan 48109, USA [5]Department of Biostatistics, University of Michigan, Ann Arbor, Michigan 48109, USA [6]Department of Radiation Oncology, University of Michigan, Ann Arbor, Michigan 48109, USA [7]University of Groningen, University Medical Center Groningen, Department of Pulmonary Diseases, Groningen, the Netherlands

Abstract

The management of bronchiolitis obliterans syndrome (BOS) following hematopoietic cell transplantation (HCT) presents many challenges, both diagnostically and therapeutically. We have developed a computed tomography (CT) voxel-wise methodology termed Parametric Response Mapping (PRM) that quantifies normal parenchyma (PRM^{Normal}), functional small airway disease (PRM^{fSAD}), emphysema (PRM^{Emph}) and parenchymal disease (PRM^{PD}) as relative lung volumes. We now investigate the use of PRM as an imaging biomarker in the diagnosis of BOS. PRM was applied to CT data from four patient cohorts: acute infection (n=11), BOS at onset (n=34), BOS

Corresponding Author: Craig J. Galban, Ph.D., Assistant Professor, University of Michigan, Radiology Department, BSRB, Room D206, 109 Zina Pitcher Place, Ann Arbor, MI 48109-2200, Phone (office): 734-764-8726, Fax: 734-615-1599, cgalban@med.umich.edu.

AUTHORSHIP CONTRIBUTIONS:
CJG, designed and performed the research, analyzed data, wrote the manuscript. JLB, processed and analyzed data, wrote the manuscript. MB, processed and analyzed data. CLK, analyzed data, wrote the manuscript. DRC, analyzed data. TDJ, statistical analysis. VL, designed research. EDT, provided data on control subjects. MVDB, provided data on control subjects. AR, designed and performed the research. EK, designed and performed the research, wrote the manuscript. MP, collected clinical data on subjects. BDR, designed and performed the research. GAY, designed the research, collected clinical data, analyzed data, wrote the manuscript.

CONFLICTS OF INTEREST: BDR and CJG have a financial interest in the underlying patented University of Michigan technology which was licensed to Imbio, LLC., a company in which BDR and AR have a financial interest. There are no other author conflicts of interest.

plus infection (n=9), and age-matched, non-transplant controls (n=23). Pulmonary function tests and broncho-alveolar lavage (BAL) were used for group classification. Mean values for PRM^{fSAD} were significantly greater in patients with BOS (38±2%) when compared to those with infection alone (17±4%, p<0.0001) and age-matched controls (8.4±1%, p<0.0001). Patients with BOS had similar PRM^{fSAD} profiles, whether a concurrent infection was present or not. An optimal cut-point for PRM^{fSAD} of 28% of the total lung volume was identified, with values >28% highly indicative of BOS occurrence. PRM may provide a major advance in our ability to identify the small airway obstruction that characterizes BOS, even in the presence of concurrent infection.

INTRODUCTION

Pulmonary complications, both infectious and non-infectious, are a common cause of morbidity and mortality following hematopoietic cell transplantation (HCT). Within this context, bronchiolitis obliterans syndrome (BOS) remains particularly problematic, characterized clinically by fixed airflow obstruction of small airways and pathologically by progressive circumferential fibrosis of terminal bronchioles. BOS is extremely heterogeneous in its presentation, due in part to the non-uniform diagnostic criteria that have been historically used to define the condition.[1,2,3] The development of NIH Consensus criteria (NIH-CC) over the past decade has been a major advance in our recognition and categorization of the disorder.[2,4] NIH-CC defined clinical parameters for the diagnosis of BOS depend upon a combination of clinical and radiographic findings, including diminished forced expiratory volumes in 1 second (FEV1), evidence of air trapping on high resolution CT (HRCT), the absence of active pulmonary infection, and the presence of chronic graft versus host disease (cGVHD) in another organ. Using the NIH-CC definition, the criteria for BOS are often not met until a patient exhibits significant airway obstruction, with FEV1 values typically less than 60% predicted at the defined onset.[3,5] Once present, the prognosis of affected patients is poor, with 5-year overall survival <20%.[5] Therapeutic options for BOS are minimal, with responses measured as disease stabilization, rather than functional improvement.[6,7] Early recognition of the disorder, prior to the development of irreversible airway changes, may potentially lead to improvements in therapeutic responses and overall survival.

The Parametric Response Map (PRM) technique has been developed at our center as a quantitative imaging biomarker for the assessment of obstructive lung disease. PRM is a voxel-based approach that provides detailed information on disease phenotype otherwise unattainable by conventional CT-based quantitative measures. Using biphasic (inspiratory and expiratory) HRCT, PRM is able to determine the severity, phenotype, and spatial heterogeneity of the pulmonary pathology using a methodology distinct from other CT-based measures[8–11]. PRM was first demonstrated on HRCT data from patients with chronic obstructive pulmonary disease (COPD), allowing quantification of the degree of functional small airway disease (fSAD) and emphysematous changes in relation to normal lung parenchyma.[8] Commonly used CT metrics for the diagnosis of lung disease have historically used tissue volumetric summary statistics of lung fields, including the mean lung density (MLD). PRM, however, classifies local variations in lung function based on a voxel-by-voxel comparison of lung attenuation changes from co-registered inspiratory and expiratory

CT scans, providing both a global and localized evaluation of lung pathology. We now report on the application of PRM to patients with BOS following HCT, specifically adapted to quantify the relative contribution of fSAD in affected individuals irrespective of the presence of acute infection. A comparison of PRM in patients with BOS, at the time of initial diagnosis of BOS (based upon NIH-CC), and during episodes of secondary infection, is now examined.

METHODS

Retrospective clinical data, pulmonary function analysis, and HRCT images at inspiration and expiration were obtained from three groups of HCT recipients at the University of Michigan Medical Center: (Group 1) Infection, no BOS; (Group 2) BOS, no Infection; and (Group 3) BOS, with Infection. Group 1 patients were early post-HCT (< 120 days), with an acute infectious pneumonitis and no clinical or radiographic features of BOS. Group 2 patients were selected at the time of NIH-CC defined onset of BOS, without active pulmonary infection. Group 3 patients were those that had previously met the NIH-CC for BOS, but now exhibited an infectious pneumonitis. Bronchoalveolar lavage (BAL) studies, including BAL special stains, PCR assays for viral pathogens, and cultures for bacteria, fungi, viruses and mycobacteria were performed to establish the presence (or absence) of an infectious pneumonitis in group 1–3 patients. Pulmonary function tests (PFT's) including measurements of FEV1, forced vital capacity (FVC), FEV1/FVC ratio, residual volume (RV) and lung diffusion capacity (DLCO) were obtained, with measurements expressed as percent predicted values. Modified NIH-CC were required to establish the diagnosis of BOS, including a FEV1 < 75% predicted, signs of obstructive airway disease (FEV1/FVC ratio < 0.7, RV > 120% predicted or evidence of air trapping on HRCT), absence of infection, and the presence of chronic graft versus host disease (GVHD) in another organ.[4] NIH lung function scores were determined, based upon published methodology.[4] Bronchoscopy was performed within 14 days (Group 1) or 28 days (Groups 2 and 3) from the defined HRCT. Pulmonary function tests were performed within 28 days of the HRCT in group 2 and 3 patients. Paired PFT's and HRCT were not available in group 1 patients, given the early post-transplant time course of this group. FEV1, FEV1/FVC and DLCO were acquired as part of the study design and analyzed in this study. In addition, a single case from Group 2 was identified as having 5 interval CT examinations. This data was analyzed and presented to demonstrate the use of PRM to monitor pulmonary complications and disease progression. All transplant subjects signed an IRB-approved informed consent for data collection and analysis.

Additional age-matched, non-transplant, healthy subjects (Group 4) were analyzed for this study to serve as negative controls (n=23). These subjects, accrued as part of a separate clinical trial at the University Medical Center Groningen (NORM Study, NCT00848406), were individuals >40 years of age who did not smoke during the last year, and had <0.5 pack years smoking history. Pulmonary function measurements (FEV1 and FEV1/FVC) were acquired on all age-matched control subjects.

Parametric Response Maps (PRM)

The PRM method consists of three key steps: image acquisition, image processing and voxel classification (Figure 1).[8]

Image Acquisition—Internal CT data at the University of Michigan were obtained as whole lung volumetric CT scans at full inspiration (total lung capacity) and incremental scans at relaxed expiration (functional residual capacity) on GE scanners (GE Healthcare) and reconstructed using a bone reconstruction kernel. Slice thicknesses were 1.25 mm for all scans with slice numbers on average around 220 and 15 for inspiration and expiration scans, respectively. All CT scans were linearly Hounsfield unit (HU)-corrected based on aortic blood (50 HU) and central air (−1000 HU) as described in previous publications.[12]

NORM Study CT data (for control subjects) were obtained as whole lung volumetric acquisitions both at full inspiration and forced expiration (residual volume) on a Siemens Somatom scanner (Siemens) with 1 mm slice thickness and a reconstruction index of 0.7 mm. A standard kernel (B30f) was used for image reconstruction. HU values of aortic blood (37 HU) and central air (−995 HU) were determined to check for scanner drift on all NORM data. All data was found to have negligible drift; as such no HU corrections were performed.

Image Processing—Image processing consisted of lung parenchymal segmentation followed by deformable volumetric registration, which spatially aligns the inspiration scan to the expiration scan such that both share the same spatial geometry. The lungs from expiratory CT scans acquired at the University of Michigan were segmented from the surrounding anatomy (i.e. bronchus, heart and chest wall) using in-house algorithms developed in a mathematical programming language (Matlab). User verification and manual corrections were applied as necessary. Whole-lung volumetric inspiration data were registered to the interval expiration data allowing presentation of the PRM maps. Inspiratory scans were co-registered to expiratory scans for all subjects and time points. Image registration was performed using a cost function of mutual information and thin-plate spline warping deformations.[13] Upon completion of image registration, the images share the same geometric space. Each voxel, the smallest unit of volume in a 3-dimensional image data set, consisted of a pair of HU values; one HU value at inspiration and another HU value at expiration. For reference, air and water attenuation values are −1000 and 0 HU, respectively.

The NORM trial acquired whole lung volumetric CT scans at both inspiration and expiration, with CT data processed by our group as described above. One distinction between the CT scans from the NORM trial and CT scans from Group 1, 2, and 3 subjects was the direction of scan registration (geometric alignment), given differences in spatial arrangements between inspiratory and expiratory views. In the NORM study, expiration scans were registered (aligned) to the inspiration scans[8], whereas CT scans for Group 1, 2 and 3 subjects did the converse, aligning the inspiratory scans with the expiration scans.

Voxel Classification—Classification of the voxels from attenuation maps into discrete zones allows quantification of normal lung parenchyma, functional small airway disease, emphysema and parenchymal disease characteristic of infection (Figure 1)(Table 1). Three thresholds are used to classify individual voxels into one of four categories with the

following color-codes: emphysema (red voxels); fSAD (yellow voxels); normal parenchyma (green voxels); and parenchymal disease (purple voxels). Voxels with HU values <−950 on the inspiration scan and ≥ −856 on the expiration scan have been identified previously as having a weak correlation to pulmonary function (i.e. FEV1).[8] As such no analysis will be performed on this measure. In addition, parenchymal tissue with voxel values above −500 HU on the inspiration scan were not analyzed in this study. Global PRM measures were calculated by normalizing the sum of all voxels within a classification by the total lung volume, which include all parenchymal voxels over the full range of HU. The nomenclature of these measures for normal lung parenchyma, functional small airway disease, emphysema and parenchymal disease were PRM^{Normal}, PRM^{fSAD}, PRM^{Emph}, and PRM^{PD}, respectively. Thresholds of −950 HU and −856 HU on the inspiration and expiration scans, respectively, were defined as specified by the COPDGene Study.[14] The upper limit on the inspiration CT (−810 HU) was determined using inspiration CT scans from the age-matched controls (Group 4; n=23) obtained from the NORM Study. Briefly, the CT lung density data was normalized by taking its natural logarithm. A bi-Gaussian fit was performed on the normalized CT data and the 95% confidence interval (1.96*standard deviation) of the principle peak that resides in a range of −1000 to −500 was determined.

Statistical Analysis

Group comparisons were determined for PRM and PFT measures using an analysis of variance (ANOVA) controlling for multiple comparisons using a Bonferroni post-hoc test. A Receiver Operating Characteristic (ROC) analysis was performed for correlation of PRM^{fSAD} with subjects diagnosed with BOS. Only subjects from Group 1 (Infection alone; n=11) and Group 2 (BOS alone; n=34) were used in this analysis. A more rigorous evaluation of PRM^{fSAD} as an indicator of BOS was performed using a discriminant analysis with leave-one out cross-validation using Group 1 and Group 2. The discriminant analysis was used to generate a predictive model for classifying subjects in Groups 1 and 2 into two predicted groups. An additional ROC analysis was then employed using PRM^{fSAD} as an independent variable and the new predicted dichotomized variable to determine an optimal cutoff for indicating BOS. Results were considered statistically significant at the two-sided 5% comparison-wise significance level ($P<0.05$). All data are presented as the mean ± SEM. All statistical computations were performed with a statistical software package (IBM SPSS Statistics, v. 21).

RESULTS

CT and PFT data were acquired from 77 patients, including 54 patients who underwent HCT at the University of Michigan, and 23 control (non-transplant) subjects (TABLE 2). Group 1 subjects (Infection, n=11) underwent CT a median of 63 days (range 19 – 109) post-HCT. Infections in Group 1 subjects included *aspergillus* (n=5), *Rhizopus* (n=2), *Fusarium* (n=1), *Cytomegalovirus* (n=1), *Moraxella* (n=1), *Herpes hominis virus* 6 (HHV6)(n=1) and *Pneumocystis jirovecii* (n=1), with multiple pathogens identified in two patients. Group 2 subjects (BOS, no infection) were selected at the time the NIH-CC for BOS were met (n=34), undergoing CT a median of 638 days (range 199 to 1545) post-HCT. Group 3 subjects (BOS + infection) (n=9) all had previously met the NIH-CC for BOS, but now

exhibited an infectious pneumonitis, undergoing CT a median of 970 days (range 259 to 3940) post-HCT. Infections in Group 3 subjects included *aspergillus* (n=5), *Pseudomonas* (n=2), and *non-tuberculi Mycobacterium* species (n=2). Infections in this group were typically sub-acute in nature, without acute infectious symptomatology (fevers, chest pain, productive cough). Group 4 patients consisted of age-matched, non-transplant controls, with FVC and FEV1 values above 100% predicted in these subjects.

The ability of PRM to characterize pulmonary pathology is demonstrated in representative axial PRM images from age-matched controls (Figure 2A), and three individuals with pulmonary complications following HCT, including an acute infectious pneumonitis (Figure 2B), BOS at NIH-CC defined onset (Figure 2C), and BOS with concurrent infection (Figure 2D). PRM classified voxels as parenchymal disease (PRM^{PD}, purple in Figure 2B and 2D) with relative volumes approximately 30% of the total lung volume in these figures. Subjects diagnosed with BOS, irrespective of the presence of infection, were identified as having extensive non-emphysematous air trapping as indicated by PRM^{fSAD} (yellow in Figure 2C and 2D). Parenchyma in a healthy control subject was identified as being normal by PRM (PRM^{Normal}, green Figure 2A).

PRM from the control subjects were similar to those observed in our previously published work.[8] In contrast, reduced levels of normal lung parenchyma (PRM^{Normal}) were noted for all three transplant groups ($p<0.0001$) (Figure 3). Mean PRM^{fSAD} were increased in subjects with BOS, in both Group 2 (38±2%) and Group 3 (35±3%). The mean PRM^{fSAD} for Group 2 and 3 subjects was significantly higher than Group 1 (17±4%, $p<0.01$) subjects and age-matched controls (8.4±1%, $p<0.0001$). There was no significant difference in mean PRM^{fSAD} between subjects in Group 2 and Group 3, p=NS. Mean PRM values for parenchymal lung disease (PRM^{PD}) were 17±2% in Group 2 (BOS, no infection) and 11±2% in age-matched controls ($p<0.001$). Although the mean PRMPD was higher in Group 1 (30±4%) vs Group 3 (20±2%) patients, the difference was not significant, p=0.08. There was also no significant difference in the level of PRM^{PD} between Group 2 and Group 3 subjects, potentially due to the sub-acute nature of the infections in the Group 3 patients. PRM^{Emph} a measure for severe emphysematous changes, was < 5% for all 3 subject groups. Significant differences in mean PRM^{Emph} levels were only observed between Group 1 and 2 patients with mean PRM^{Emph} 0.3% and 4.0% respectively, p=0.04.

We analyzed the predictive potential of PRM^{fSAD} in identifying subjects with BOS (Group 2; n=34) from those with acute pulmonary infection (Group 1; n=11). We first used an ROC analysis to correlate PRM^{fSAD} with the likelihood that an individual would have BOS. PRM^{fSAD} was found to significantly identify BOS with an area under the curve (AUC) of 0.861 ($p<0.001$) and 95% confidence intervals of 0.743 and 0.979. We next performed a discriminant analysis with leave-one out cross-validation that provided a more rigorous test of PRM^{fSAD} as an indicator of BOS., Through the discriminant analysis, we again found PRM^{fSAD} to be a significant predictor of BOS with sensitivity and specificity of 0.76 and 0.72, respectively ($p<0.0001$). Out of all cross-validated grouped cases, 75% were correctly classified. To determine an optimal cutoff, an ROC analysis of PRM^{fSAD} using the newly classified data from our discriminant analysis generated an optimal PRM^{fSAD} cutoff of 28% of the total lung volume, with values > 28% indicative of BOS. This PRM^{fSAD} cut-point

(>28%) remained a valid indicator of BOS, irrespective of the presence (or absence) of a concurrent infection.

Serial PRM measurements

The potential ability of PRM to identify significant fSAD in patients, prior to fulfillment of the NIH-CC for BOS, is shown in Figure 4. In this patient, PRM imaging from a HRCT obtained one year post-HCT revealed PRM^{fSAD} of 41%, with 17% PRM^{PD}. The NIH-CC for BOS would not be fulfilled, however, until nearly 3 years post-HCT. During this same period, PRM^{fSAD} levels continued to increase, peaking at 3 years post-HCT at 65%, with PRM^{Normal} decreasing from 27% to 13% over the same time period. The subject subsequently underwent a lung allograft approximately 7 years post-HCT for management of his end-stage lung disease. As anticipated, PRM^{Normal} values increased significantly after the lung allograft, from 13% to 54% of the total lung volume (Figure 4).

DISCUSSION

We demonstrate the utility of PRM, a voxel-based imaging technique applied to paired inspiratory and expiratory CT lung scans, to serve as a diagnostic index of fSAD following HCT. Elevated levels of PRM^{fSAD} were present in patients with BOS, even in the setting of concurrent pulmonary infection. An optimal cut-point for PRM^{fSAD} of 28% of the total lung volume was identified, with values > 28% highly indicative of BOS. In addition, by retaining spatial information within the lung parenchyma, PRM provides a unified methodology that can simultaneously identify and quantify the extent of fSAD within the lungs. Quantitative PRM measures can be tracked temporally, providing real-time diagnostic information on the progression of fSAD that could be acted upon by the treating physician.

BOS is currently defined by NIH-CC in which obstructive airway disease (by radiographic and spirometric parameters) plus absence of active lung infection are required to establish the diagnosis. The application of the NIH-CC can be challenging, given the frequent infectious complications that affected patients often exhibit post-HCT. Recurrent infections in this patient population hinder our diagnostic capabilities, with patients often meeting NIH-CC for BOS only after severe airflow abnormalities are already present. This is an important problem, since once a patient is diagnosed with BOS, overall survival is poor, < 20% at 5-years.[15] The ability of PRM to identify significant elevations in fSAD, even in the setting of an active infection, may lead to earlier recognition of BOS, and subsequent treatment interventions.

The role of PRM as an imaging biomarker for detection of BOS will require validation in larger case series and may ultimately complement known diagnostic markers for disease. A number of novel biomarkers for early BOS detection, including serologic and BAL fluid biomarkers have been recently reported in lung allograft and HCT recipients, including the glycoprotein YKL-40, hypoxia inducible 1 alpha (HIF-1α), and various metalloproteinases.[16–18] In lung allograft recipients, BAL fluid levels of interleukin-15 (IL-15), interleukin-17 (IL-17), tumor necrosis factor alpha (TNFα), and α1-antitrypsin were predictive of BOS development in one report,[17] with over-expression of interleukin-8 (IL-8), lung surfactant proteins A and D (SP-A and SP-D), and BAL fluid neutrophil levels

predictive of BOS in other reports.[18,19] Non-invasive biomarkers, including measurement of fractional exhaled nitric oxide (FeNO) may additionally serve a role in early BOS detection.[20] Given the heterogeneity of the disorder, with complexities in both diagnosis and management, a panel of both invasive and non-invasive biomarkers may be required for diagnosis and risk classification of patients.

The current study focuses on the application of PRM in patients with BOS following HCT. The study was not designed to examine PRM within specific infections, nor examine the role of PRM in other non-infectious pneumonitis post-HCT, including idiopathic pneumonia syndrome (IPS), restrictive lung disease (RLD) and cryptogenic organizing pneumonia (COP). Fungal pathogens were the predominant pathogen in both Group 1 (Infection, no BOS) and Group 3 (BOS, with Infection) patients, with a paucity of bacterial (n=3) and viral pneumonitis (n=2) present within the study population. In addition, the current study did not find significant differences in fSAD levels between Group 2 (BOS, no infection) and Group 3 (BOS, with infection), both groups exhibiting > 30% mean PRM^{fSAD}. This is an important finding to note, as increased levels of fSAD were thus present in patients with BOS, regardless if a concurrent infection were present or not.

BOS exhibits a wide spectrum of phenotypes, characterized by a lymphocytic bronchitis and small airway inflammation early in the clinical course, with subsequent fibrinous obliteration of bronchiolar lumen developing later in the disease.[21,22] The histologic changes are often heterogeneous in nature, with varying degrees of involvement within segments of individual lobes. Correlation of lung histology with PRM values was limited in the current trial, with surgical lung, or transbronchial biopsies performed in only 6 of the 34 Group 2 patients. The spatial information gathered by PRM may ultimately help clinicians identify (and target) optimal sites for biopsy and lavage, during diagnostic bronchoscopic procedures.

Although CT is widely used for diagnosis and staging of various lung disorders, a lack of consensus has brought about various acquisition protocols and reconstruction algorithms between CT scanners. In general, the best clinical practice for the use of CT in diagnosing BOS is to use a well-calibrated, high-resolution CT and to apply consistent acquisition and reconstruction parameters. PRM may provide disparate results from multiple-time-point CT examinations that do not take precautionary measures to avoid inconsistencies in acquisition and reconstruction parameters. Nevertheless, image post-processing can be performed to minimize fluctuations in HU values between similar CT examinations (e.g. acquired at full inspiration, consistent lung histograms). We, as others, find that HU values can be corrected to minimize effects from scanner drift.[12,23] This procedure for correcting datasets allows the use of archival data in many cases. Even low-resolution interval expiration scan data produce reliable PRM results. Using a separate cohort of CT data, we determined that the insertion of gaps (max 10 mm gap) in whole-lung volumetric expiration CT data only generated differences of 1.6% from the high-resolution (contiguous) PRM analysis (unpublished results). Nevertheless, HU-based measurements using widely spaced axial slices have the potential to misrepresent disease classification, particularly when the disease is spatially heterogeneous.

There are other limitations in the current study that must be addressed. The first is the retrospective nature of sample collection, resulting in the use of varying CT protocols on an inter-patient basis. Despite the great care that was taken to minimize intra-patient variability in CT protocols and reconstruction algorithms, there were some cases where patient CT acquisitions and reconstruction algorithms varied slightly. As described previously, additional analyses were performed to investigate the sensitivity of PRM measurements to low-resolution interval expiration CT scans and reconstruction algorithms. In addition, we have previously tested the effect of different registration directions on the PRM results. Again using a separate cohort of whole-lung volumetric inspiration and expiration CT data, we found that registering to the expiration scans overestimates the amount of PRM^{fSAD} in absolute terms by approximately 5% when compared to PRM results from registrations to the inspiration scans (unpublished data). Although beyond the scope of this study, a more thorough analysis is necessary to fully ascertain the limits of the PRM analytical approach.

This is the first trial to investigate the role of PRM in characterizing BOS post-HCT. Many questions remain. Is there a more optimal PRM^{fSAD} cut-point for identifying BOS, one with a higher sensitivity and specificity than currently exhibited? Can PRM provide earlier detection of BOS than standard spirometry, prior to any significant decline in FEV1 or FEV1/FVC? Can a PRM signature for BOS be validated in a multi-center trial, in which centers have applied varying CT acquisition techniques? Does a PRM signature exist for other pulmonary complications post-HCT, potentially differentiating infectious from non-infectious pulmonary complications? Ultimately, PRM requires testing in a multi-site clinical trial consisting of highly characterized subjects with detailed longitudinal data collection, including spirometric measurements, in order to validate this work in both BOS and other post-transplant lung complications.

In conclusion, PRM provides a quantitative imaging analysis for patients with BOS following HCT, with elevated levels of fSAD present in affected patients. The ability for PRM to both quantify and spatially define the severity of lung airway disease in patients with BOS may serve as a major advance in the diagnosis and management of this disorder.

Acknowledgments

We’d like to thank Ms. Verica Saveski and Ms. Sandra Klaus for their administrative assistance with this project. This work was supported by the US National Institutes of Health research grants P50CA93990 and P01CA085878. J.L.B. is a recipient of support from the US National Institutes of Health training grant T32EB005172.

REFERENCES

1. Afessa B, Litzow MR, Tefferi A. Bronchiolitis obliterans and other late onset non-infectious pulmonary complications in hematopoietic stem cell transplantation. Bone Marrow Transplantation. 2001; 28(5):425–434. [PubMed: 11593314]
2. Williams KMCJ, Gladwin MT, Pavletic SZ. Bronchiolitis obliterans after allogeneic hematopoietic stem cell transplantation. JAMA. 2009; 302(3):306–314. [PubMed: 19602690]
3. Au BK, Au MA, Chien JW. Bronchiolitis obliterans syndrome epidemiology after allogeneic hematopoietic cell transplantation. Biol Blood Marrow Transplant. 2011 Jul; 17(7):1072–1078. [PubMed: 21126596]
4. Filipovich AH. Life-threatening hemophagocytic syndromes: current outcomes with hematopoietic stem cell transplantation. Pediatr Transplant. 2005 Dec; 9(Suppl 7):87–91. [PubMed: 16305623]

5. Chien JW, Duncan S, Williams KM, Pavletic SZ. Bronchiolitis obliterans syndrome after allogeneic hematopoietic stem cell transplantation-an increasingly recognized manifestation of chronic graft-versus-host disease. Biol Blood Marrow Transplant. 2010 Jan; 16(1 Suppl):S106–S114. [PubMed: 19896545]
6. Hildebrandt GC, Fazekas T, Lawitschka A, et al. Diagnosis and treatment of pulmonary chronic GVHD: report from the consensus conference on clinical practice in chronic GVHD. Bone Marrow Transplant. 2011 Mar 28.
7. Yanik G, Kitko C. Management of noninfectious lung injury following hematopoietic cell transplantation. Curr Opin Oncol. 2013 Mar; 25(2):187–194. [PubMed: 23340330]
8. Galban CJ, Han MK, Boes JL, et al. Computed tomography-based biomarker provides unique signature for diagnosis of COPD phenotypes and disease progression. Nat Med. 2012 Nov; 18(11): 1711–1715. [PubMed: 23042237]
9. Gevenois PA, De Vuyst P, de Maertelaer V, et al. Comparison of computed density and microscopic morphometry in pulmonary emphysema. Am J Respir Crit Care Med. 1996 Jul; 154(1):187–192. [PubMed: 8680679]
10. Gorbunova V, Lol P, Ashraf H, Dirksen A, Nielsen M, de Bruijne M. Weight preserving image registration for monitoring disease progression in lung CT. Med Image Comput Comput Assist Interv. 2008; 11(Pt 2):863–870. [PubMed: 18982686]
11. Matsuoka S, Kurihara Y, Yagihashi K, Hoshino M, Watanabe N, Nakajima Y. Quantitative assessment of air trapping in chronic obstructive pulmonary disease using inspiratory and expiratory volumetric MDCT. AJR Am J Roentgenol. 2008 Mar; 190(3):762–769. [PubMed: 18287450]
12. Stoel BC, Stolk J. Optimization and standardization of lung densitometry in the assessment of pulmonary emphysema. Investigative radiology. 2004 Nov; 39(11):681–688. [PubMed: 15486529]
13. Meyer CR, Boes JL, Kim B, et al. Demonstration of accuracy and clinical versatility of mutual information for automatic multimodality image fusion using affine and thin-plate spline warped geometric deformations. Medical image analysis. 1997 Apr; 1(3):195–206. [PubMed: 9873906]
14. Regan EA, Hokanson JE, Murphy JR, et al. Genetic epidemiology of COPD (COPDGene) study design. COPD. 2010 Feb; 7(1):32–43. [PubMed: 20214461]
15. Chien JW, Sakai M, Gooley TA, Schoch HG, McDonald GB. Influence of oral beclomethasone dipropionate on early non-infectious pulmonary outcomes after allogeneic hematopoietic cell transplantation: results from two randomized trials. Bone Marrow Transplant. 2010 Feb; 45(2): 317–324. [PubMed: 19561649]
16. Jaksch P, Taghavi S, Klepetko W, Salama M. Pretransplant serum human chitinase-like glycoprotein YKL-40 concentrations independently predict bronchiolitis obliterans development in lung transplant recipients. J Thorac Cardiovasc Surg. 2014 Feb 26.
17. Fisichella PM, Davis CS, Lowery E, Ramirez L, Gamelli RL, Kovacs EJ. Aspiration, localized pulmonary inflammation, and predictors of early-onset bronchiolitis obliterans syndrome after lung transplantation. Journal of the American College of Surgeons. 2013 Jul; 217(1):90–100. discussion 100–101. [PubMed: 23628225]
18. Ditschkowski M, Elmaagacli AH, Koldehoff M, Gromke T, Trenschel R, Beelen DW. Bronchiolitis obliterans after allogeneic hematopoietic SCT: further insight--new perspectives? Bone Marrow Transplant. 2013 Sep; 48(9):1224–1229. [PubMed: 23435515]
19. Kennedy VE, Todd JL, Palmer SM. Bronchoalveolar lavage as a tool to predict, diagnose and understand bronchiolitis obliterans syndrome. Am J Transplant. 2013 Mar; 13(3):552–561. [PubMed: 23356456]
20. Neurohr C, Huppmann P, Leuschner S, et al. Usefulness of exhaled nitric oxide to guide risk stratification for bronchiolitis obliterans syndrome after lung transplantation. Am J Transplant. 2011 Jan; 11(1):129–137. [PubMed: 21087415]
21. Urbanski SJ, Kossakowska AE, Curtis J, et al. Idiopathic small airways pathology in patients with graft-versus-host disease following allogeneic bone marrow transplantation. The American Journal of Surgical Pathology. 1987; 11:965. [PubMed: 3318513]

22. Cooke, KR.; Yanik, G. Lung injury following hematopoietic stem cell transplantation. In: Appelbaum, FR.; Forman, SJ.; Negrin, RS.; Blume, KG., editors. Thomas' Hematopoietic Cell Transplantation. 4th ed. Wiley-Blackwell; 2009.

23. Tanabe N, Muro S, Hirai T, et al. Impact of exacerbations on emphysema progression in chronic obstructive pulmonary disease. Am J Respir Crit Care Med. 2011 Jun 15; 183(12):1653–1659. [PubMed: 21471102]

Key Points

Parametric Response Mapping (PRM) serves as an imaging biomarker that quantifies and spatially defines the presence of BOS following HCT.

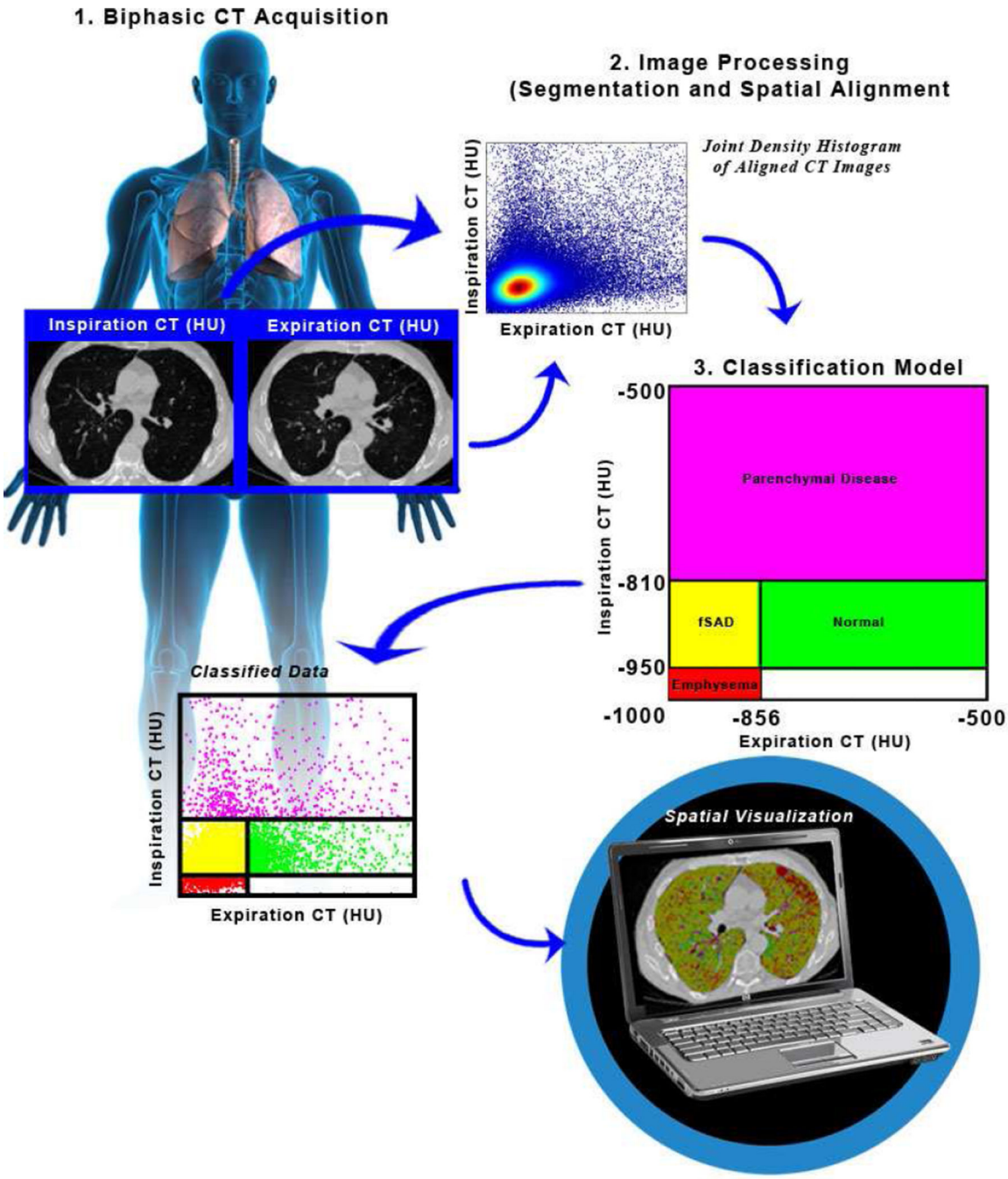

Figure 1.
Schematic diagram of the PRM workflow.

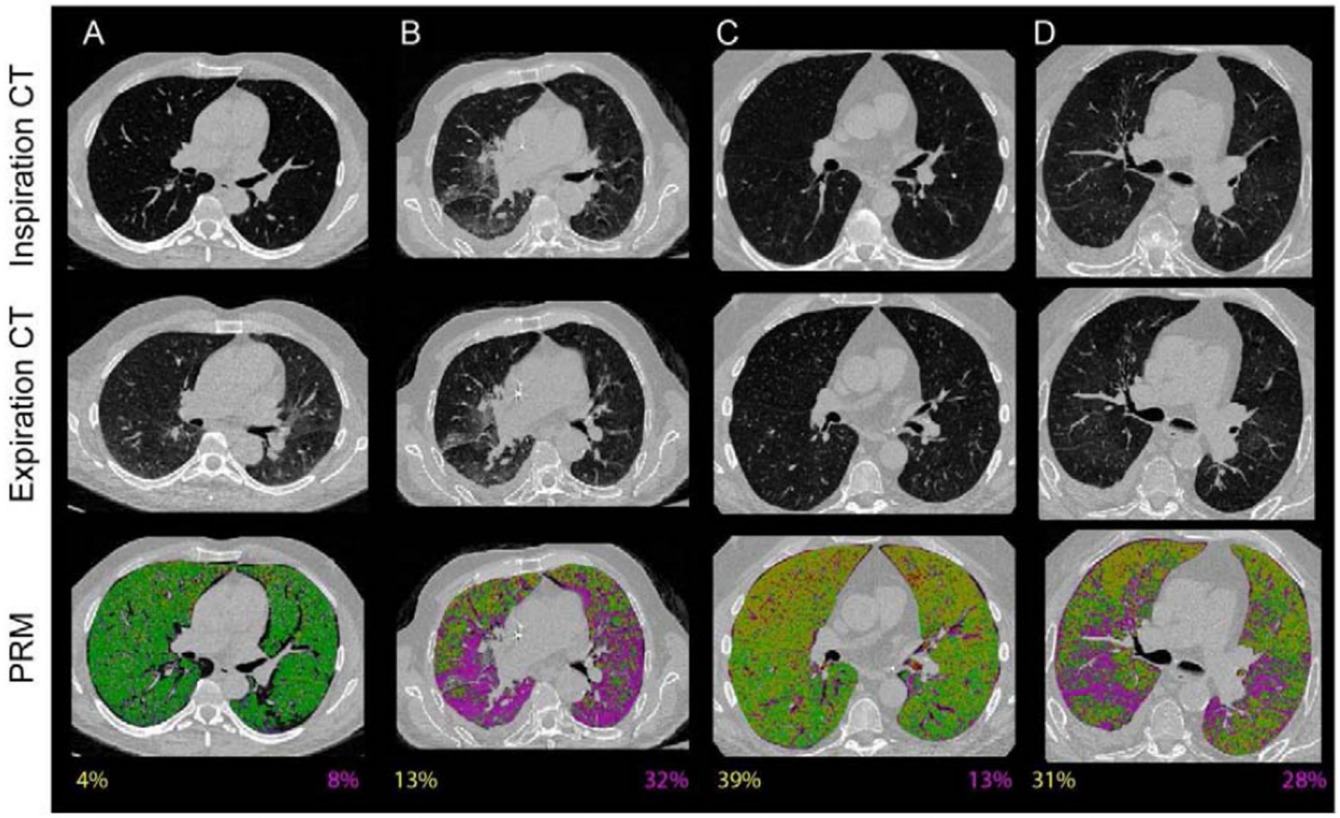

Figure 2.

A–D: Pulmonary complications identified by PRM. Normal lung tissue is denoted green (PRM^{Normal}), functional small airway disease yellow (PRM^{fSAD}), emphysematous changes red (PRM^{Emph}), and parenchymal disease purple (PRM^{PD}). PRM^{fSAD} and PRM^{PD} values are provided at the bottom of PRM images (values are color-coded to disease component). (**A**) Healthy age-matched, non-transplant control. (**B**) Fungal pneumonitis, 61 days post-HCT. (**C**) BOS at NIH-CC defined onset, 448 days post-HCT. No concurrent infection present. (**D**) *Pseudomonas* pneumonitis in a patient with previously documented BOS, now 447 days post-HCT.

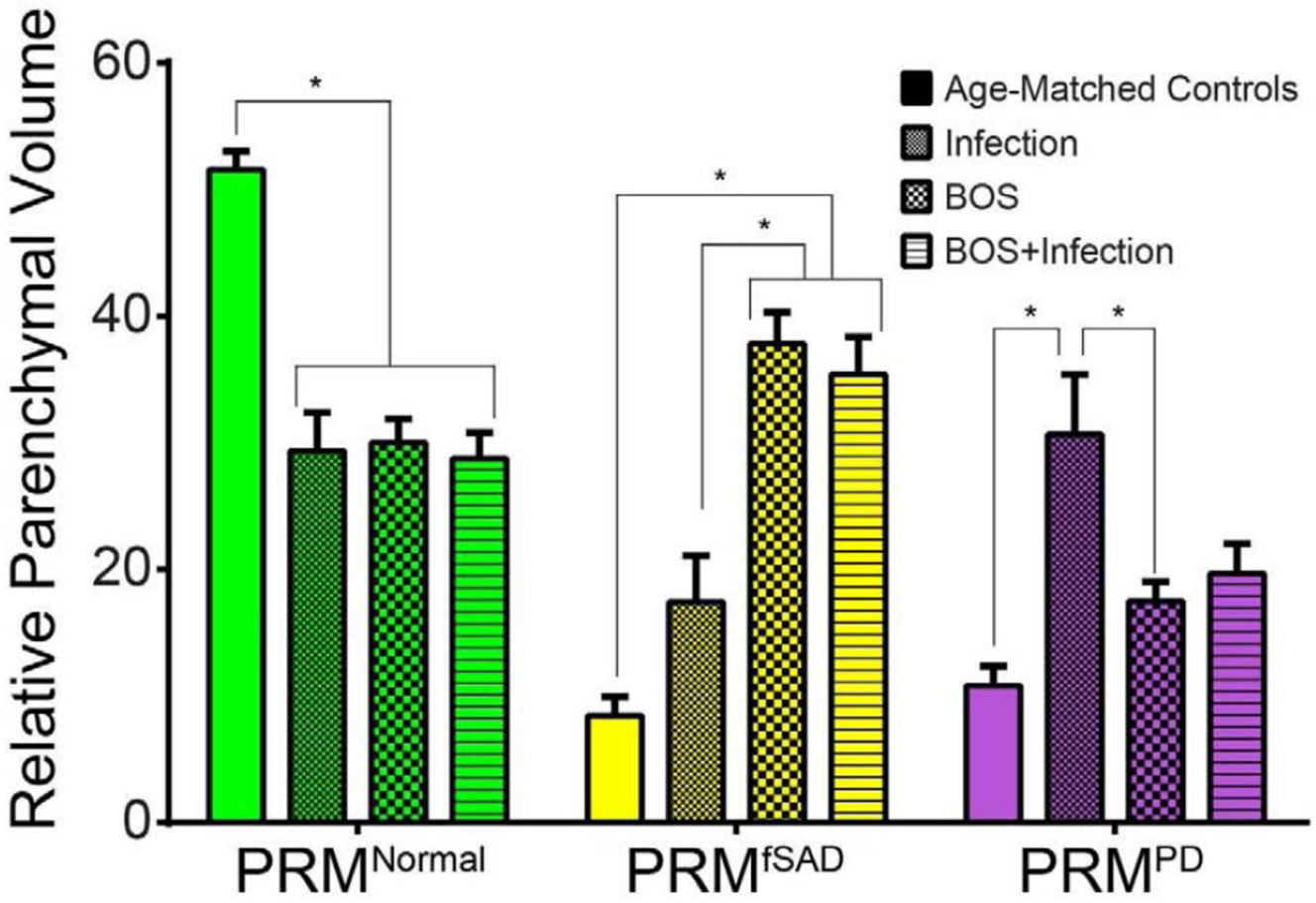

Figure 3.

Group comparisons in pulmonary function measures and PRM. Bar plots are used to present the group differences observed in PRM measurements, PRM^{Normal}, PRM^{fSAD} and PRM^{PD}. Statistical significance was assessed at $p<0.05$ and denoted by *. Data is presented as the mean ± SEM.

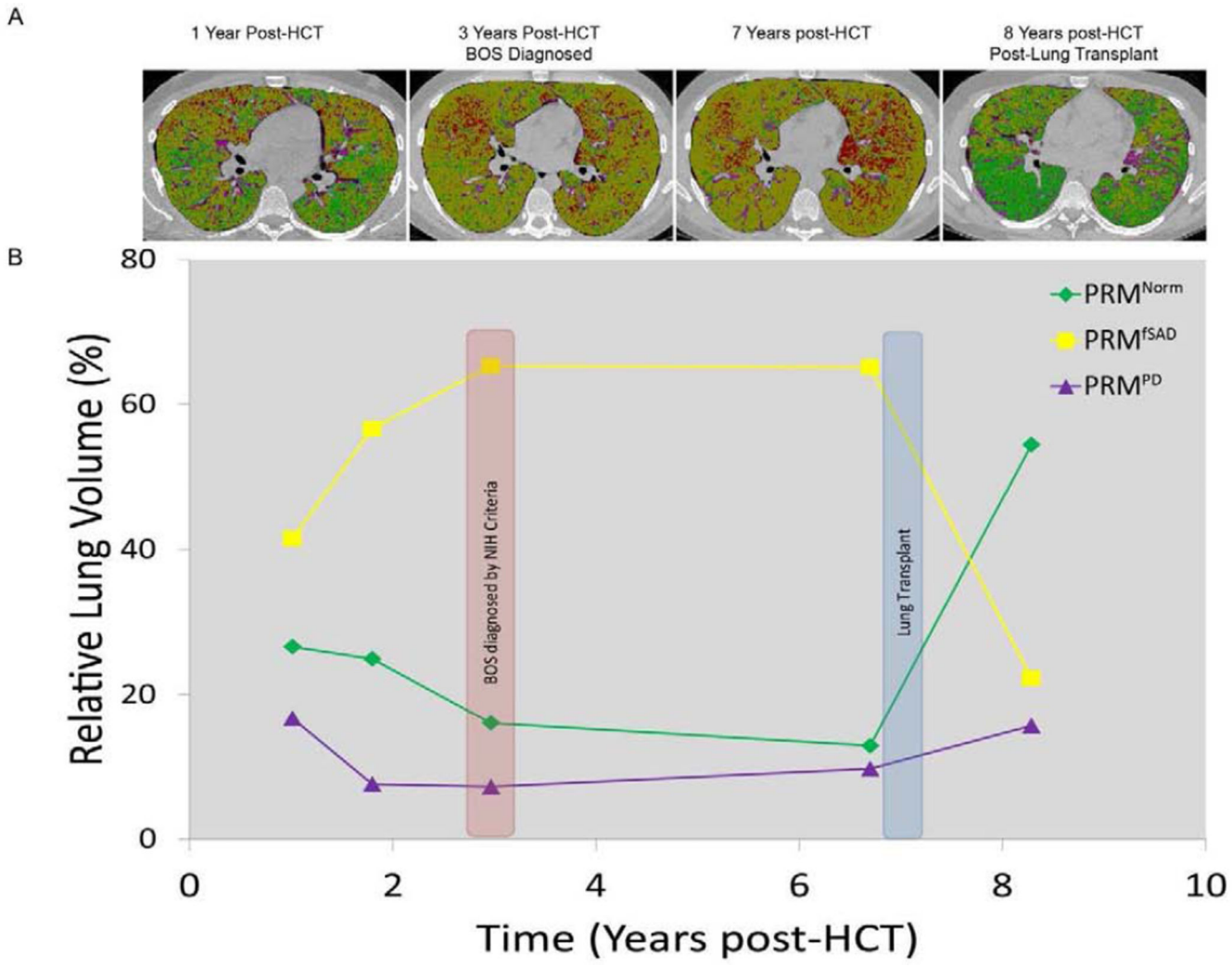

Figure 4.

Onset and progression of BOS post-HCT in a single patient. (**A**) Representative PRM axial slices are provided at discrete time points following HCT. (**B**) Line plot with axes time (years) and PRM relative lung volumes (%) at various time points post-HCT.

Table 1

Classification schema, based upon attenuation maps.

	PRM^{Emph}	PRM^{fSAD}	PRM^{PD}	PRM^{Normal}
Inspiration	−1000≤ to <−950 HU	−950≤ to <−810 HU	−810≤ to <−500 HU	−950≤ to <−810 HU
Expiration	−1000≤ to <−856 HU	−1000≤ to <−857 HU	−1000≤ to <−500 HU	−856≤ to <−500 HU

Biol Blood Marrow Transplant. Author manuscript; available in PMC 2015 October 01.

Table 2

Demographics.

		Group 1 (Infection)	Group 2 (BOS)	Group 3 (BOS + Infection)	Controls
Total patients		11	34	9	23
Age (years)					
	Median	58	54	53	57
	Range	38–68	12–69	30–69	44–73
Gender					
	Males/Females	10/1	16/18	3/6	16/7
Disease					NA[4]
	AML/MDS	3	21	4	
	ALL	1	5	0	
	Lymphomas	5	2	3	
	Myeloma	2	2	2	
	CML	0	4	0	
Days post-transplant					NA
	Median	63	638	970	
	Range	19–109	199–1545	259–3940	
Pulmonary Function Test[1]					
	FVC (median %) NA[2]		72	64	111
	FEV1 (median %)	NA	46	38	119
	DLCO (median %)	NA	54	49	NA
NIH Lung Function scores[3]		72			
	Median	NA	8	9	NA
	Range	NA	3–12	5–12	

Key:

[1], Values expressed as percent predicted.

[2], PFT's were not obtained at the time of HRCT for group 1 patients.

[3]. NIH Lung Function scores per Filipovich et al, ref 4.

[4]. Controls were healthy non-transplant subjects, non-smokers, no underlying malignancy.